Collision-induced friction in the motion of a single particle on a bumpy inclined line

S. Dippel,[1] G. G. Batrouni,[1,2] and D. E. Wolf[1]
[1]*Höchstleistungsrechenzentrum, Forschungszentrum Jülich, D-52425 Jülich, Germany*
[2]*Groupe Matière Condensée et Materiaux, URA CNRS 804, Université de Rennes 1, 35042 Rennes Cedex, France*
(Received 11 March 1996; revised manuscript received 2 July 1996)

By means of molecular-dynamics simulations, we investigate the elementary process of avalanches and size segregation by surface flow in two dimensions: a single ball confined to moving along an inclined line consisting of balls. The global characteristics of the motion depend strongly on the size of the moving ball relative to the size of the balls on the line, as well as the distribution of the balls on the line. We find that in the steady state the friction force acting on the ball is independent of material properties such as the Coulomb friction coefficient and the coefficient of restitution. Contrary to previous notions about the details of the motion, we find that it is very regular and consists of many small bounces on each ball on the line. As a result of this regularity, introducing a random spacing between the balls on the line has mainly the same influence as a regular spacing of adequate length. The insensitivity of the steady-state velocity to material properties and to the detailed arrangement of the balls on the line allows for an analytical estimation of the mean velocity that fits the simulation results very well. We find that results from the two-dimensional case can probably not be transferred to the three-dimensional case of a ball moving on a rough inclined plane as easily as has been suggested previously. [S1063-651X(96)00912-9]

PACS number(s): 46.90.+s, 07.05.Tp, 46.30.Pa, 83.70.Fn

I. INTRODUCTION

The flow of granular materials has been studied extensively both experimentally and theoretically due to its ubiquity in nature and its industrial importance. Nevertheless, many properties of granular flow are still poorly understood. Here we deal with a special case of granular flow, namely, that along an inclined rough surface. Examples are flow in inclined chutes [1] and all kinds of avalanche processes, such as rockslides [2], which involve segregation (known as ''inverse grading'' to geologists), an important phenomenon often encountered in granular materials [3]. In rotating drums, avalanche processes are the motor of size segregation [4–7]. Segregation in surface flow is strongly related to the question of stability of granular flow on rough surfaces, i.e., to the determination of the limiting conditions for the existence of a steady state where the flow is neither stopped nor accelerated. The rougher the surface encountered by the moving particles, the slower they flow, and they may even come to a stop. Thus the larger the flowing particles are compared to the roughness or bumpiness of the surface on which they flow, the farther they should travel and accumulate (in the case of flow on a sand heap) at the bottom of the slope.

The threshold for the onset of granular shear flows and the limiting conditions for which a stable flow (i.e., a steady state) still exists are insufficiently understood and hard to determine in realistic situations [8]. In particular, the hysteretic properties of granular materials, manifesting themselves, for example, in the difference between the static and dynamical angle of repose of sandpiles [9], complicate the situation. Though the static threshold for the onset of motion on a rough plane (i.e., the tilt of the surface large enough to set a resting mass of granular material in motion) has been quite thoroughly investigated in experiments and computer simulations [10,11], the dynamical case, i.e., the stability of the flow, is still poorly understood.

In order to investigate the dynamical situation, we follow the course taken up by Riguidel *et al.* [11–13] in their experimental studies. We consider the elementary process of an avalanche: a single ball of radius R moving down an inclined plane onto which other balls of radius r are glued. This fixes the roughness of the surface. Such a system has been investigated experimentally and numerically in three dimensions (i.e., for a ball moving on a plane) [11,12,14] and in two dimensions (for a ball moving on a line of balls) [13,15]. The simulations in three dimensions were restricted to the determination of the static angle of stability for a ball resting on the plane, whereas all experiments and the simulations on the line also dealt with the dynamical situation of a ball that starts on the plane with some initial velocity, which is the situation we are interested in.

In all cases, three types of motion could be observed, depending on the size ratio $\Phi = R/r$ and on the inclination angle θ of the plane. These results could be summed up in a ''phase diagram'' (typical for both the plane and line), for which we will later give an example from our simulations. The three types of motion observable in experiments and simulations are characterized in the following way. In regime A, the ball gets trapped on the plane independently of the initial velocity with which it is launched onto it. In regime B, it reaches a constant average velocity $\overline{v}$ in the direction along the plane. In regime C, it accelerates throughout the whole length (2 m in the experiments) of the plane, accompanied by visible jumps. In the constant velocity regime, the mean velocity $\overline{v}$ was found to be proportional to $\Phi^{\alpha}\sin\theta$ in three dimensions, with an exponent $\alpha \approx 1.3$ [11,12,14], whereas in two dimensions $\overline{v^2}$ depended linearly on $\sin\theta$ [15,16]. In two dimensions, no simple power law could be found for the Φ dependence of the mean velocity. The relation $\overline{v^2} \sim \sin\theta$ was already derived using very general assumptions by Bagnold for flow of many particles on an inclined plane [17], but no assumption about the

dimensionality of the system was made there.

An obvious difference between the two-dimensional (2D) and 3D case is the fact that in three dimensions, the particle moving down the plane will be deflected in the direction perpendicular to the plane inclination either by rolling down the crooked valleys formed by the balls on the plane or by obliquely impacting a sphere on the plane. We will return to the importance of this possibility, which is absent from the simulations we present here, after having discussed the details of the motion of the ball moving down the line. Recently, a 2D stochastic model has been proposed that reproduces the angle dependence of the velocity in three dimensions, but gives a different exponent α [18].

Here we discuss the mechanism by which the ball keeps a constant velocity on the inclined *line* and how, from the understanding of this mechanism, the transition to the stopping and accelerating regime can be explained. We will show that the 2D case is *qualitatively* different from the 3D case, i.e., that the effect of disorder on the plane cannot be modeled by disorder on a line. Possible reasons for the success and the adequateness of the 2D stochastic model of Ref. [18] in describing the 3D case are discussed.

The outline of the paper is as follows. After presenting our simulation method in Sec. II, we will show in Sec. III that the simulations reproduce experimentally observed macroscopic behavior, which we will discuss qualitatively. We then proceed to a detailed analysis of the microscopic properties of the motion and give an explanation of the mechanism stabilizing the motion of the ball in the two-dimensional case. The influence of material properties on the motion is investigated. On the basis of our simulation results, we present in Sec. IV a simplified model for the motion of the ball that allows the analytical derivation of the mean velocity in the two-dimensional case. The results of this model agree with the simulation results. Possible reasons for the difference between the two-dimensional and the three-dimensional system are discussed.

II. SIMULATION METHOD

We model the 2D case by the molecular-dynamics (MD) technique [19], which was introduced to the simulation of granular materials by Cundall and Strack [20]. The MD technique consists of time-integrating Newton's equations of motion for a system of grains starting from a given initial configuration. Since our simulations are two dimensional, the grains have only three degrees of freedom, two translational, one rotational. Two grains of radii R_i, positions $\vec{r}_i$, velocities $\vec{v}_i$, and angular velocities ω_i $(i=1,2)$ are in contact when their (virtual) overlap $\xi = \max(0, R_1+R_2-|\vec{r}_2-\vec{r}_1|)$ is larger than zero (''soft'' grains). Two unit vectors $\vec{n}$ and $\vec{s}$ are used to decompose the forces and velocities into normal and shear components

$$\vec{n}=\frac{\vec{r}_2-\vec{r}_1}{|\vec{r}_2-\vec{r}_1|}, \tag{1}$$

$$\vec{s}=((\vec{n})_y,-(\vec{n})_x). \tag{2}$$

The forces between grains are then given by

$$\vec{F}_{ij}=F_n\vec{n}+F_s\vec{s}, \tag{3}$$

where

$$F_n=-k_n\xi-\gamma_n\dot{\xi}, \tag{4}$$

$$F_s=-\min(|\gamma_s v_s|,|\mu F_n|)\,\mathrm{sgn}(v_s). \tag{5}$$

Here μ denotes the Coulomb friction coefficient. The relative normal velocity v_n and the relative shear velocity v_s (i.e., the relative velocity of the surfaces at the point of contact) are defined as

$$v_n=(\vec{v}_2-\vec{v}_1)\cdot\vec{n}, \tag{6}$$

$$v_s=(\vec{v}_2-\vec{v}_1)\cdot\vec{s}+\omega_1R_1+\omega_2R_2. \tag{7}$$

A number of different force laws is commonly used in MD simulations of granular materials; a discussion of their properties can be found in [21]. Our choice of F_n corresponds to a simple linear spring dashpot; the tangential force F_s is the Coulomb friction law for sliding friction, which was regularized for small v_s to avoid the discontinuity of the Coulomb law at $v_s=0$. The tangential damping constant γ_s should have a sufficiently high value such that the case $F_s=-\gamma_s v_s$ occurs only for very small v_s. Only then does the interpretation of F_s as a mere regularization of Coulomb friction hold. This force law has the advantage of holding equally well in free impacts of spheres [21,22] and in long-lasting contacts [23] if the particles can be considered as rough hard spheres (i.e., if tangential elasticity can be neglected). It also gives a velocity-dependent coefficient of tangential restitution, a feature found to be important in a stochastic model of the situation [18,24].

Throughout our simulations we used the parameters $k_n=2\times10^6$ N/m, $\gamma_s=100$ kg/s, $\mu=0.13$, $r=5$ mm, and $M=\frac{4}{3}\pi R^3\rho$ for the mass of the rolling ball with $\rho=7.8$ g/cm^3. The values of these parameters were chosen to match the steel balls used in [13,16]; the choice of k_n leads to a collision time of the order of 10^{-5} s, which is a typical value for steel balls of this size. The value of γ_s is high enough such that F_s is reasonably close to the exact Coulomb friction law in the sense explained above. The damping γ_n is determined by fixing the normal coefficient of restitution $e_n=-v_n^f/v_n^i$, defined by the ratio of final and initial normal velocities. Unless stated otherwise, the results presented in Sec. III were obtained using $e_n=0.7$ and the above-mentioned parameters. The influence of the material parameters e_n and μ on the behavior of the system will be discussed later. The only external force acting on the ball is gravity; the gravitational acceleration in the x (y) direction is given by $g\sin\theta$ $(-g\cos\theta)$. The integration method we employ is a constant-time-step fifth-order predictor-corrector method [19].

Figure 1 shows a schematic drawing of the ball on the line. The spacing between two balls fixed on the line is $2\epsilon r$, where ϵ is a number that in the disordered case is chosen uniformly distributed in the interval $[0,\epsilon_{\max}]$. The *impact angle* γ is defined as the angle enclosed by the line joining the centers of the impacting balls and the normal to the

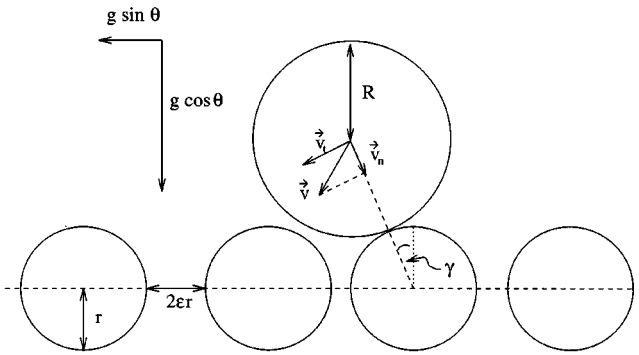

FIG. 1. Schematic drawing of the ball on the line.

plane. It is taken to be negative when the ball collides with the uphill facing side of a ball on the plane, positive on the downhill side.

III. SIMULATION RESULTS

A. Global characteristics of the motion

In all simulations presented here, the ball was launched onto the line with a rather high velocity v_x in the x direction and quite low v_y. If the inclination angle θ and size ratio $\Phi = R/r$ are in a suitable range, the moving ball very quickly, usually after passing only a few balls on the line, reaches a steady state with well-defined mean velocities in the x and y directions. Clearly, the average over v_y is zero in our problem, so the only interesting *mean* velocity is the average over v_x, which we denote by $\overline{v}$. To obtain this mean velocity, we first average over a certain number of time steps (usually 500). This value is large enough to average out the comparably large fluctuations occurring during collisions, while it is still so small that the ball moves only a very short distance (much less than the radius of the balls on the line) during this time. This averaged value clearly still gives a fluctuating velocity, but the fluctuations are very small and $\overline{v}$, the mean value of these averaged velocities, is well defined.

We investigated the motion of the ball both on lines with equally spaced balls and on lines with randomly spaced balls. We found that the essential features of the motion are alike in both cases. Figure 2 shows the velocity of the rolling

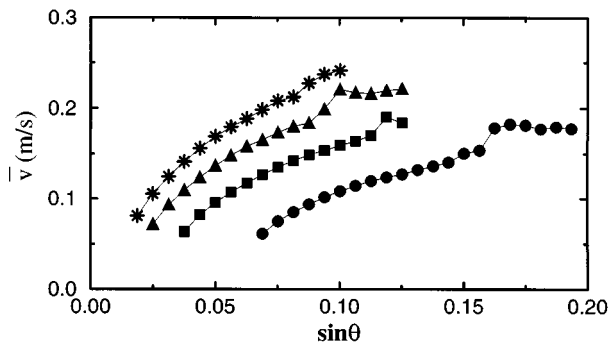

FIG. 2. Dependence of the mean velocity $\overline{v}$ on the inclination of the line for various size ratios Φ: $\Phi = 1.5$ (circles), $\Phi = 2.0$ (squares), $\Phi = 2.5$ (triangles), and $\Phi = 3.0$ (stars).

ball for various Φ and equal spacing of balls on the line with $\epsilon = 0$ as obtained from simulations using the above-mentioned parameters. For the case $\epsilon = 0$, experimental data are available (though only for size ratios $\Phi \leqslant 2.0$) [13,16]. Our stable mean velocities are of the same order of magnitude, but in the simulations the range of inclination angles for which $\overline{v}$ is well defined, i.e., a steady state is reached, is a bit narrower than in the experiments. This might be due to the difference in the experimental setup. There, a ball moved down a line of balls sitting in a V-shaped groove, and it is to be expected that contact with the groove walls influenced the motion as an additional source of dissipation due to friction and collisions with the walls, but it is unclear how strong this influence was. For a direct comparison of simulation and experiment, it would be desirable that a ''more'' two-dimensional experiment be done, such as, for example, a ball moving down a row of cylinders, to rule out these boundary effects.

For angles lower than the one for which the smallest steady-state velocity is reached for a given Φ, the ball loses all the initial velocity it had and very quickly stops, usually after passing only very few balls on the line (which defines region A of the phase diagram). We will denote this minimum angle, for which a steady state with $\overline{v} \neq 0$ still exists, by $\theta_{AB}(\Phi)$. This defines the phase boundary between regions A and B.

All velocity curves in Fig. 2 exhibit a sudden increase of $\overline{v}$ to a value where it remains roughly constant. This sudden increase has also been observed in experiments [13]. For angles smaller than the one where this happens, the velocity of the ball shows only very small fluctuations and the steady-state velocity $\overline{v}$ does not depend on the initial velocity of the ball. At the inclination angle where the velocity suddenly shoots up, the behavior changes qualitatively. The fluctuations of v_x increase significantly and the behavior of the ball now depends on the initial velocity. Depending on the starting velocity, the ball can accelerate (usually if the starting velocity is larger than the stable mean velocity) and start to jump visibly, or it can reach a constant velocity (if released with an initial velocity smaller than the stable $\overline{v}$ in this region). However, even when the ball does not accelerate, in this region $\overline{v}$ can depend somewhat on the initial velocity. We thus denote the angle at which the sudden increase takes place by $\theta_{BC}(\Phi)$ since it defines the upper boundary of the constant velocity region B independently of the initial velocity of the ball.

If θ increases even more, the ball accelerates and starts to jump significantly (the length and height of the jumps reach a few ball diameters). We did not investigate this jumping motion any further, for the following two reasons. In the simulations the ball accelerated up to 50 m/s and more, which is a velocity the ball would never reach in experiments due to air resistance. Thus the question of whether the ball in the jumping regime can reach a steady state only due to collisions with the plane will not be discussed here, even though it is of theoretical interest. The second reason is that for grazing impacts at high velocities, an artifact of constant-time-step algorithms, the so-called brake failure effect [25] may set in, which leads to anomalous dissipation of energy. Its onset can be shifted to higher velocities by increasing the spring constant k_n, i.e., the stiffness of the balls. This, how-

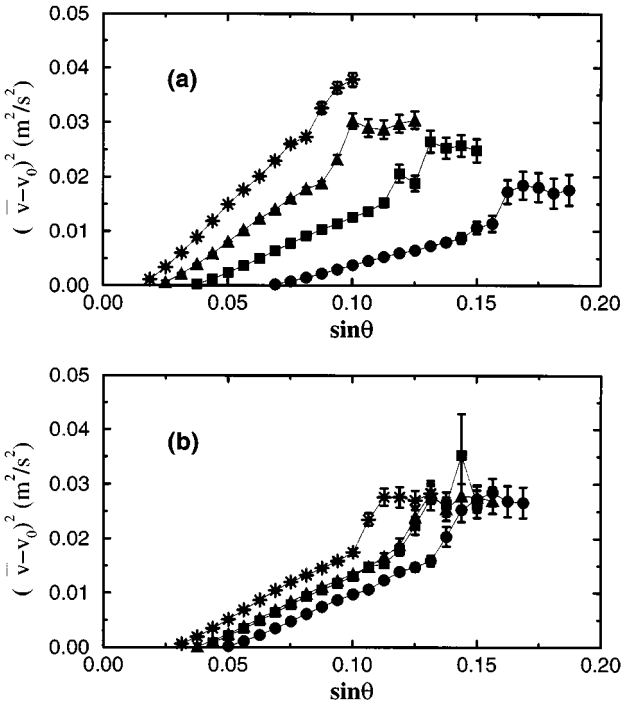

FIG. 3. Dependence of $(\overline{v}-v_0)^2$ on the inclination of the line for (a) the same parameters as Fig. 2 and (b) various spacings of the balls on the line ($\Phi=2.25$): balls equally spaced with $\epsilon=0$ (stars), $\epsilon=0.1$ (triangles), and $\epsilon=0.2$ (circles) and balls disordered with $\epsilon_{\max}=0.2$ (squares).

ever, decreases the time step, thus increasing the simulation time tremendously. The constant-time-step algorithm then becomes a very ineffective way of simulating the motion, since the ball spends most of its time in free flight, where a time step small enough to integrate collisions correctly and to avoid spurious effects is essentially a waste of computation time. In this regime, event-driven (ED) simulations would be more appropriate, which is why we will not discuss the motion in the ''high-bounce'' regime. One might argue that since the ball moves down the line in a series of bounces, an ED algorithm might in any case be a more efficient and appropriate way to simulate the motion. As we will see later, this is not the case, as both short- and long-lasting contacts occur, the latter of which are not treatable by an ED algorithm in a straightforward way [26].

The velocity curves obtained from experiments as well as from simulations suggest the functional form

$$\overline{v}=v_0(\Phi)+f(\Phi)\sqrt{\sin\theta-\sin\theta_{AB}(\Phi)} \tag{8}$$

for a fixed value of r in region B. All curves start at a certain offset velocity v_0, which seems to depend slightly on Φ. $f(\Phi)$ denotes a (still unknown) scaling function, which, unlike in three dimensions, does not seem to be a simple power law. We thus plot $[\overline{v}-v_0(\Phi)]^2$ in Fig. 3, where $v_0(\Phi)$ is obtained by fitting a square root to $\overline{v}(\sin\theta)$. $v_0(\Phi)$ typically is of the order of 4 cm/s. The error bars give the variance of the averaged velocities, averaged (as the plotted value of $\overline{v}$ itself) over a number of simulation runs with different starting velocities. Figure 3(a) shows velocities in the case

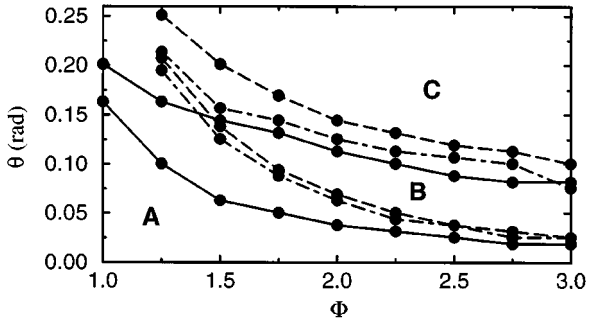

FIG. 4. Phase diagram for $e_n=0.7$ and various spacings of the balls on the line: balls equally spaced with $\epsilon=0$ (solid line) and $\epsilon=0.2$ (dashed line) and balls disordered with $\epsilon_{\max}=0.2$ (dot-dashed line).

$\epsilon=0$ for various size ratios and Fig. 3(b) illustrates the influence of disorder on the velocity of a ball of size ratio $\Phi=2.25$.

Figure 3(b) demonstrates how the velocity of the ball is affected by the introduction of disorder to the line. It shows that $\overline{v}$ on the disordered line with $\epsilon_{\max}=0.2$ can be approximated by the velocity on a line with equally spaced balls and a spacing $\epsilon=0.1$, corresponding to the mean value of the disordered case. It also shows that $\theta_{BC}(\Phi)$ depends on both Φ and the arrangement of the balls on the line, whereas the maximum $\overline{v}$ only seems to depend on Φ.

In Fig. 4 we plot the corresponding phase diagram for three cases: two cases for a line with balls equally spaced, with $\epsilon=0$ and $\epsilon=0.2$, and the third for a disordered line with $\epsilon_{\max}=0.2$. The lines denote the phase boundaries given by the angles $\theta_{AB}(\Phi)$ and $\theta_{BC}(\Phi)$ defined previously. Obviously, the introduction of disorder has the same effect on the phase boundary AB as the introduction of an equal spacing of balls with $\epsilon=\epsilon_{\max}$. This is understandable; the stopping of a ball should be ruled by the deepest ''traps'' into which it might fall. The boundary BC rather seems to be determined by the mean spacing of balls since in the disordered case it falls somewhere between the two extreme cases of an ordered array with $\epsilon=0$ and $\epsilon=\epsilon_{\max}$.

B. Detailed dynamics of the motion

In order to investigate the mechanism by which the ball maintains a constant velocity in region B, we have to look into the details of the motion. Certainly, distributions of the impact angle γ, of times of flight between impacts, or of the impact velocity $\vec{v}^i$ would be of interest. One might ask as well if there are correlations between impacts at certain angles and the corresponding impact velocities or between the time of flight after an impact and the corresponding impact angle. Actually, these correlations provide even more detailed information; for this reason we will examine them first. We will first discuss the ordered case of a line with no spacing between the balls, i.e., with $\epsilon=0$.

In Fig. 5 we plot the velocity of the ball right before an impact as a function of the corresponding impact angle γ. Each dot corresponds to a collision. We chose to plot the normal velocity v_n and the tangential *translational* velocity

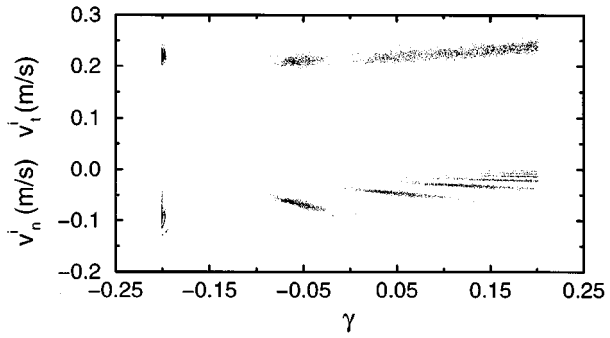

FIG. 5. Correlation of impact velocities and impact angles γ (in radians) for $\Phi=4$, $\sin\theta=0.05$, and $\epsilon=0$. The upper points correspond to the relative translational tangential velocity $v_t=\vec{v}\cdot\vec{s}$, the lower ones to the relative normal velocity v_n.

$v_t=\vec{v}\cdot\vec{s}$ rather than v_x and v_y, as they provide more information on the mechanisms involved. Since dissipation takes place only through the normal velocity (dissipation due to F_s is negligible, as we will see later), the evolution of this quantity may explain the mechanism of energy loss maintaining the steady state. Since v_t is the velocity component of the motion of the center of mass of the ball along the bumps of the surface, it reflects how this bumpiness is felt. It is obvious that there is a strong correlation between the impact angles and the corresponding impact velocities. The times of flight between impacts and corresponding previous impact angles are equally strongly correlated (see Fig. 6). From both Figs. 5 and 6 it is obvious that the ball moves down the line in a series of bounces. There is even a certain range of impact angles that are never hit. In addition, we can deduce from Fig. 6 that the typical times of flight between impacts correspond to a distance of less than 3 mm, which is smaller than the radius of the balls constituting the line. So the bounces the ball undergoes cannot be very high or far and the bouncing ball collides with every ball on the line several times.

How can these results be understood? From Fig. 5 two important points can be extracted. First, we see that at certain impact angles γ, the moving ball is likely to hit the ball on the line with a well-defined corresponding normal velocity v_n, which leads to an equally well-defined time of flight (see Fig. 6). Second, the normal velocities are largest for negative

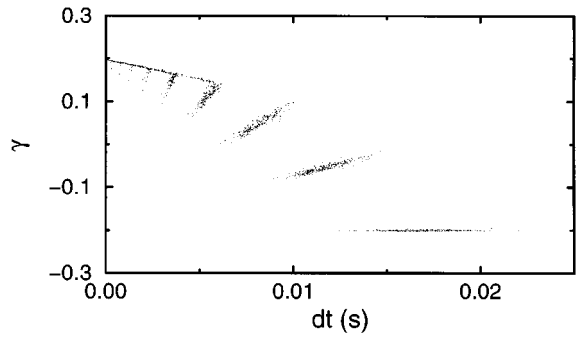

FIG. 6. Correlation of the time of flight after an impact at angle γ (in radians) and corresponding previous impact angles (the parameters are the same as in Fig. 4).

impact angles (i.e., hitting on the uphill side of a line ball) and get smaller (and eventually very close to zero) with increasing impact angles. The second observation helps to explain the correlations and reveals the reasons for the regularity of the motion.

Consider a ball that has just arrived at the maximum possible positive impact angle $\gamma_{\max}$ on a certain ball on the line, say ball number k. The value of $\gamma_{\max}$ is given by the geometry and defined as

$$\gamma_{\max}=\arcsin\frac{1+\epsilon}{1+\Phi}. \tag{9}$$

From Fig. 5 we see that at $\gamma_{\max}$ the moving ball has lost nearly all normal velocity with respect to ball k, i.e., it is rolling or sliding down the lower part of the ''downhill side'' of the corresponding ball on the line. Even though the total shear velocity v_s at the point of contact is quite small (the ball rolls, thus rotational velocity is opposed to the translational tangential velocity and nearly compensates it), the translational tangential velocity $v_t=\vec{v}\cdot\vec{s}$, which we plot in Fig. 5, is quite large (close to v for larger Φ). Immediately after having reached $\gamma_{\max}$ on ball k, the moving ball impacts the next ball, $k+1$, at $-\gamma_{\max}$, where a large part of this previously tangential velocity is now normal velocity, as the direction of the vector $\vec{n}$ connecting the centers of the impacting balls with respect to $\vec{v}$ has changed. The ball thus gets thrown up again and manages to reach the downhill side of ball $k+1$ after a few jumps. The comparably high normal velocity of the ball at $-\gamma_{\max}$ is lost in two ways in crossing a fixed ball: most is lost by dissipation due to impacts, but partly it is converted into tangential velocity by the increasing obliqueness of successive impacts at positive γ. In the process of bouncing over the top of ball $k+1$ on the line, the moving ball loses nearly all of its normal velocity, so that it again reaches $\gamma_{\max}$ with nearly only tangential velocity. These steps repeat themselves over and over again while the ball moves down the plane, thus retaining a constant mean velocity. Note that strong geometrical constraints prevent the ball from rolling down the line without ever bouncing. Whenever the moving ball rolls down the downhill side of a ball k, it is thrown onto the uphill side of ball $k+1$ with considerable normal velocity with respect to ball $k+1$ as a result of the change in the geometry. To remain in contact with ball $k+1$, the moving ball would have to lose a very substantial amount of this normal velocity in a single impact, or it would jump up. Persistent rolling thus is only possible in the case of vanishing normal restitution. Rolling on part of each ball is possible, however, as we will see in a moment.

In order to describe things more quantitatively, we take a look at the distribution of impact angles. Figure 7(a) gives an example for an angle of inclination in the middle of region B of the phase diagram for $\Phi=2.5$. The distribution exhibits clear peaks for $\gamma<0$. As γ increases, the peaks broaden somewhat and approach each other until they are nearly indistinguishable in the histogram, although there still is structure in the correlation plots. For plane inclinations closer to θ_{AB} than to θ_{BC}, the distribution, like in Fig. 7(a), even breaks off at a value $\gamma<\gamma_{\max}$, indicating the start of a long-lasting contact. Here the ball has lost so much of its normal

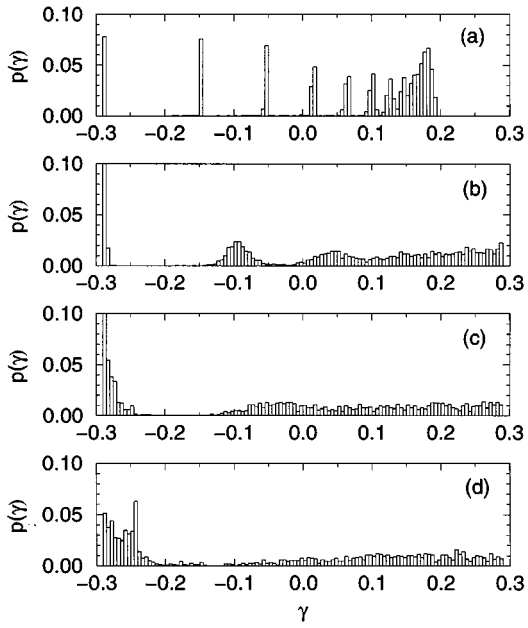

FIG. 7. Distribution of impact angles (in radians) for $\Phi=2.5$, $\epsilon=0$, and (a) $\sin\theta=0.057$, (b) $\sin\theta=0.075$, (c) $\sin\theta=0.091$, and (d) $\sin\theta=0.103$.

velocity in impacts it suffered on crossing over the top of a ball on the line that it finally starts to roll over part of this ball. This rolling motion can even start while the moving ball is still on the uphill facing side of the fixed ball, though this takes place only very close to θ_{AB}. All these impacts *end* at $\gamma_{\max}$, which leads to the very pronounced peak at $-\gamma_{\max}$. Integrating the distribution over negative and positive angles, respectively, yields the result that there are actually more impacts for positive than for negative γ.

When θ is increased, the peaks for negative γ, except the one at $-\gamma_{\max}$ move towards zero, finally disappearing into the continuous distribution for positive γ (see Fig. 8). At a large enough inclination, they get visibly broader, showing that the velocity at $\gamma_{\max}$ is now no longer as sharply defined as before, probably due to the fact that not all the normal velocity can be lost on only one ball. Still, the ball does not

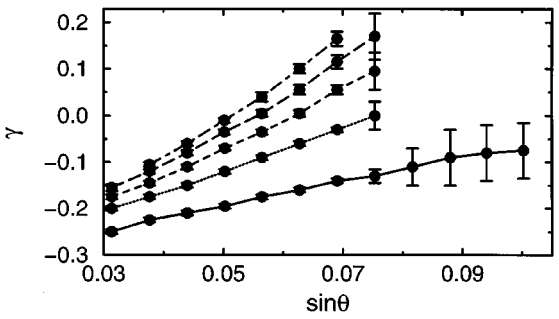

FIG. 8. Location of the peaks in the distribution of impact angles (in radians) for $\Phi=2.25$. The error bars denote the width of the peak. The solid, dotted, dashed, long-dashed, and dot-dashed lines denote, respectively, the first, second, third, fourth, and fifth distinguishable peak, excluding the one at $-\gamma_{\max}$.

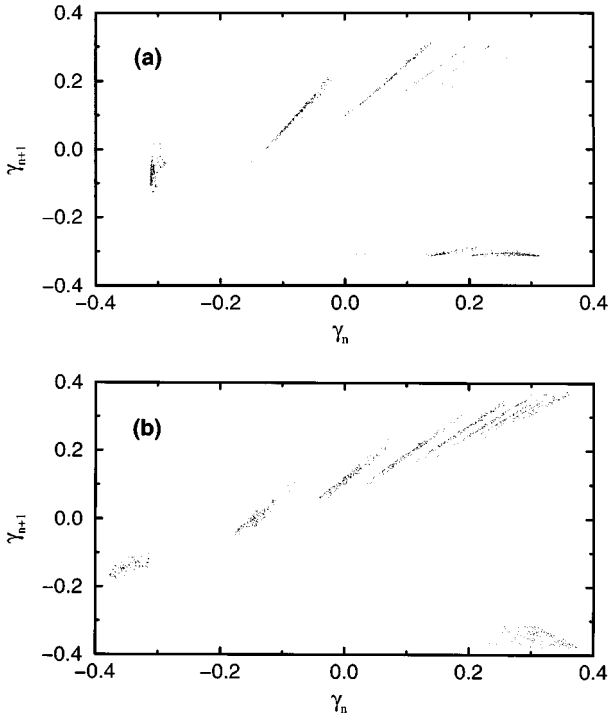

FIG. 9. Correlation of successive impact angles (in radians) for $\Phi=2.25$ and $\sin\theta=0.094$. (a) Balls on the line regularly spaced ($\epsilon=0$) and (b) balls on the line disordered with $\epsilon_{\max}=0.2$.

accelerate as long as its starting velocity is only a little higher than its stable mean velocity (this is the region beyond the transition from linear to more irregular behavior in Fig. 2).

Figures 7(b)–7(d) shows how the motion of the ball changes qualitatively at θ_{BC}. The θ values are taken a little below (b), as close as possible to (c), and a little above θ_{BC} (d). The heretofore clearly defined peak at $-\gamma_{\max}$ broadens considerably and even seems to develop a small side peak as θ reaches θ_{BC}. The qualitative change of the behavior of the ball can also be observed in the velocities. In particular, in the angle region where the velocity curve flattens out again, an intermittent behavior of the ball can be observed: it will accelerate a little, even start to jump a little, but then suddenly slow down again. The mean velocity in this case is determined by how fast the ball is accelerated and slowed down, respectively. The same intermittent behavior of the ball shortly before passing from motion with a mean constant velocity to a jumping regime has been observed in 3D experiments [16] and in a stochastic model for the 2D case [18].

While the intermittent behavior marks the transition from region B to region C in the phase diagram, stopping of the ball takes place when the typical tangential velocity at $\gamma_{\max}$ does not convert into enough normal velocity at $-\gamma_{\max}$ to carry the ball over the top of the next ball in the line in a few jumps, or at least up to a point where the remaining tangential velocity suffices to make it roll over the top of this ball. In regime B, the motion is characterized not only by typical impact angles γ, but also by a very strong correlation of successive impact angles. In Fig. 9 we plot γ_{n+1}, the impact angle for impact $n+1$ as a function of the previous impact angle γ_n. Even when introducing a random spacing of balls on the line, the strong correlation remains. This observation

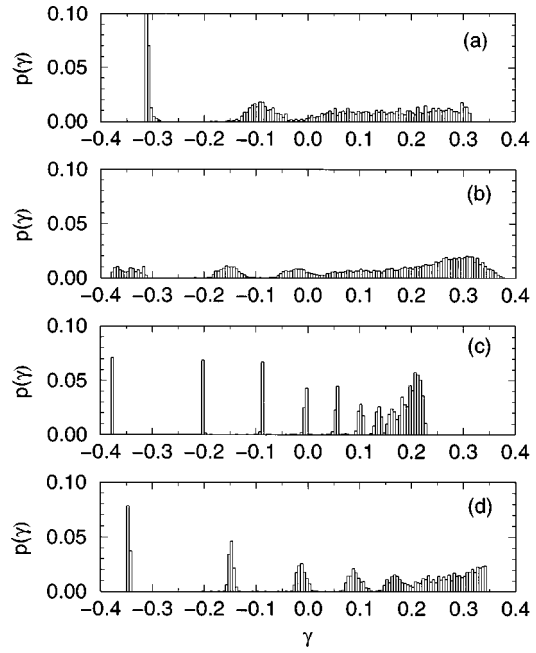

FIG. 10. Distribution of impact angles (in radians) for $\Phi=2.25$, $\sin\theta=0.088$, and various spacings of the balls on the line: (a) regular spacing, $\epsilon=0$; (b) disordered line, $\epsilon_{\max}=0.2$; (c) regular spacing, $\epsilon=0.2$; and (d) regular spacing, $\epsilon=0.1$.

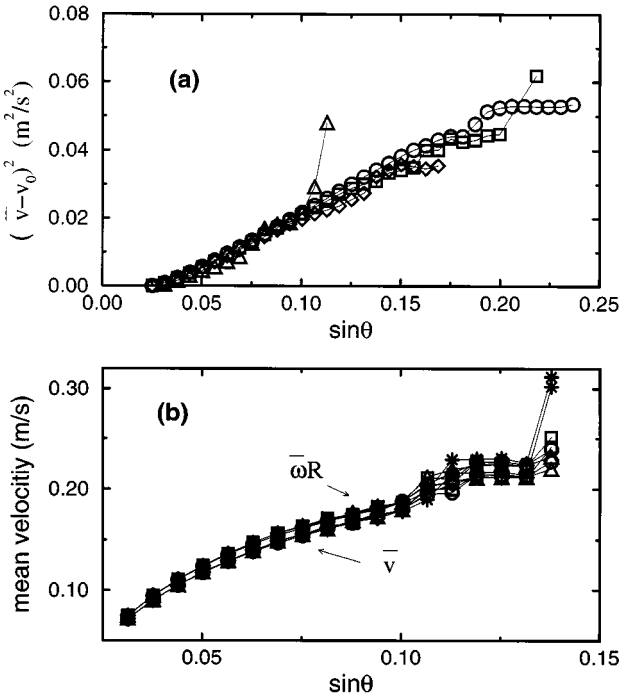

FIG. 11. (a) Dependence of $\overline{v}$ on the dissipation for $\Phi=2.25$ and $\epsilon=0$: $e_n=0.4$ (○), 0.5 (□), 0.6 (◇), and 0.8 (△). (b) Dependence of $\overline{v}$ and $\overline{\omega R}$ on the friction coefficient μ: $\mu=$ 0.1 (○), 0.3 (□), 0.5 (◇), 0.7 (△), and 1.0 (⋆).

leads us to the discussion of the behavior of the moving ball on a disordered line. The phase diagram already suggests that introducing disorder has a similar influence on the motion of the ball as the introduction of a regular spacing. In both cases, the region of stable motion in the phase diagram shifts to larger Φ and θ. Plotting the distribution of impact angles for the cases displayed in Fig. 2(b) shows the effect of disorder (see Fig. 10).

We checked that this regularity in the case of a disordered line is not a finite-size effect. The angle distributions do not change when the size of the system is increased. From Fig. 10 it can be seen that the distributions for the impact angles in the disordered case lie between the limiting cases $\epsilon=0$ and $\epsilon=0.2$ of an ordered line. In addition, the peaks for $\epsilon=0.1$ correspond to the center of the peaks in the disordered case. The reason for the large width of the peaks in the case $\epsilon=0$ lies in the fact that here the velocity is already quite high [see Fig. 2(b)]. We interpret the results of the disordered case in the following way. The motion of the ball is influenced mainly by two factors: the minimum and maximum spacing of balls on the line. If the ball is to keep its mean velocity, without being stopped and without being accelerated, the velocity has to have a value that enables it to get out of the ''deepest valleys'' existing between two balls (given by $\epsilon_{\max}$), but still is low enough that in all cases (even in those where $\epsilon=0$) most of the normal velocity is dissipated on crossing over the corresponding ball, so that at $\gamma_{\max}$ of this ball only tangential velocity is left. The variations in this tangential velocity are so small that they only broaden the peaks for the impact angles, but do not lead to a *qualitative* change of the motion of the ball.

C. Influence of material properties on the motion

Having uncovered the mechanism by which the ball moves down the line and keeps a constant average velocity, we now have to ask how much this mechanism and the global results such as $\overline{v}$ are influenced by material properties. The material properties incorporated in our simulations are the coefficient of normal restitution e_n and the friction coefficient μ. We will show in this subsection that their influence on $\overline{v}$ and the mean rotational velocity $\overline{\omega}$ is very small.

Experiments in three dimensions already indicate that the characteristics of the motion are hardly influenced by material properties [14,27]. Rolling steel, glass, and plastic balls down the plane gives nearly the same velocity, though for plastic (which has the lowest e_n and largest μ) the B region of the phase diagram is found to be somewhat extended. Our simulations in two dimensions indeed show that the mean velocity $\overline{v}$ is nearly independent of both e_n and μ. Figure 11 demonstrates this for the case of a ball of size ratio $\Phi=2.25$. Figure 11(a) shows the velocities for varying normal coefficient of restitution e_n. It can clearly be seen that e_n influences the phase diagram i.e., the extension of region B, but has only a very small influence on $\overline{v}$. Though θ_{AB} is hardly affected by e_n (except for very small Φ), θ_{BC} moves to larger inclination angles θ with decreasing e_n. But e_n influences $\overline{v}$ slightly in a direction that is contrary to what one would expect intuitively. Increasing the dissipation leads to a slight increase in the velocity. We have found no explanation for this so far. We have, however, understood the relative insensitivity of $\overline{v}$ to e_n.

The reason for the small influence of e_n is essentially the regularity of the motion. As shown in the Sec. III B, the ball moves over each line ball in a succession of bounces, in the course of which it loses all or most of its relative normal velocity with respect to this line ball. e_n mainly determines how many bounces are necessary to achieve this. As long as

the moving ball has only a negligible amount of normal velocity left as it reaches $\gamma_{\max}$, it seems to be unimportant for the tangential velocity at this point how many impacts were needed to lose the normal velocity the ball had at $-\gamma_{\max}$.

For the phase boundary BC, the value of e_n is important. Since we found that the motion of the ball starts to become unstable when the motion is no longer regular, we expect the destabilization to start when the normal velocity at $-\gamma_{\max}$ with respect to one ball cannot be lost by the time $\gamma_{\max}$ is reached. But e_n, which determines the energy loss in a collision and thus the height (and thereby the length) of the next jump, together with $\overline{v}$ determines how many jumps are made on one line ball. It thus gives an upper limit to the maximum amount of energy that can be dissipated on a single line ball. The smaller e_n, the more energy is dissipated in each jump and the more jumps are possible, as their length decreases. Thus θ_{BC} shifts to larger θ for a given Φ with decreasing e_n and approaches the static angle of stability, which in the 2D case is given by $\gamma_{\max}$.

We find that because the ball is allowed to rotate, the value of the friction coefficient μ is even less important for the behavior of the ball than e_n [see Fig. 11(b)]. μ influences neither $\overline{v}$ nor the mean rotational velocity $\overline{\omega}$ significantly. It also does not change the phase boundaries. The reason for this is that for the range of θ considered here, the ball can be expected to roll without slipping most of the time independent of μ if our implementation of the tangential force law correctly reproduces Coulomb's law for sliding friction. Let us assume for a moment that the ball, while moving down the line, is always in contact with the balls on this line, which is only possible if $e_n=0$. It would then roll without slipping if at all γ the condition $|F_s|\leqslant\mu|F_n|$ were fulfilled. For a rolling sphere under the action of gravity [28],

$$|F_s|=\frac{2}{7}|\vec{g}\cdot\vec{s}|, \tag{10}$$

so that the criterion for μ for the ball to roll without slipping reads

$$\mu>\frac{2}{7}|\tan(\theta+\gamma)|. \tag{11}$$

Though close to $\gamma_{\max}$ this condition is usually not fulfilled (the smaller Φ, the larger the region of γ for which slip can occur), it holds on the largest part of a ball on the line even for small μ. We would thus assume the ball on the average to roll without slipping in the case of $e_n=0$ even for small values of the friction coefficient μ.

In our simulations, however, we used larger values for e_n, such as $e_n=0.7$ in Fig. 11(b), so there the ball rather bounced than rolled down the line. But the distances the ball covers between bounces in the steady state are very small. We find in our simulations that the ball, which we launch onto the plane without rotational velocity, soon picks up rotation during impacts, such that when the steady state is reached, the rotational velocity has adjusted itself to a value that on average leads to zero relative velocity of the surfaces of the moving ball and the fixed balls [except close to $\gamma_{\max}$, just as would be expected from Eq. (11)]. In the free flight between collisions, the ball picks up translational velocity while the rotational velocity remains unchanged. The moving ball has thus gained excess shear velocity, which is converted nearly completely into rotation in the next impact, if it is small enough. This is usually the case in the steady state, where distances covered between bounces are small.

IV. THEORETICAL MODEL FOR THE MEAN VELOCITY

In this section, we derive $\overline{v}$ by a simple analytical treatment. Our simulation results play an important role here, as they show which simplifications can be introduced without losing essential features of the motion.

From our results on the influence of the coefficient of restitution e_n on the motion of the ball, we can deduce a very accurate result for $\overline{v}$ in the case of equally spaced balls on the line. Since we find that $\overline{v}$ hardly depends on e_n we investigate the limiting case $e_n=0$. As we also found that, due to friction, the ball is able to sustain $v_s=0$ on average (i.e., the ball would roll without slipping in the case $e_n=0$ for large μ), we make the following assumptions.

We assume that the moving ball is always in contact with the fixed balls, i.e., rolls down the line without slipping. Thus, at all times

$$|\vec{v}|=v_t=\vec{v}\cdot\vec{s}, \tag{12}$$

$$v_n=0, \tag{13}$$

$$\omega R=v_t. \tag{14}$$

From these conditions the equation of motion of the ball on a single ball on the line from $-\gamma_{\max}$ to $\gamma_{\max}$ can be derived. The kinetic energy of the ball is

$$E_{\text{kin}}=\frac{1}{2}mv_t^2+\frac{1}{2}J\omega^2, \tag{15}$$

where J denotes the moment of inertia of the moving particle, which in the case of a sphere of radius R takes the value $J=\frac{2}{5}mR^2$. Using condition (14), we get

$$E_{\text{kin}}=\frac{7}{10}mv_t^2 \tag{16}$$

for a sphere. The potential energy depends on the location of the moving ball on the line ball:

$$E_{\text{pot}}=mg(R+r)\cos(\gamma+\theta). \tag{17}$$

Since $v_t=(R+r)\dot{\gamma}$, the energy balance reads (denoting the energies at the start of the motion by E_{kin}^0 and E_{pot}^0)

$$E_{\text{kin}}^0-\frac{7}{10}m(R+r)^2\dot{\gamma}^2=mg(R+r)\cos(\gamma+\theta)-E_{\text{pot}}^0. \tag{18}$$

Differentiating with respect to time yields the equation of motion for $\gamma(t)$

$$\ddot{\gamma}=\frac{5}{7}\frac{g}{R+r}\sin(\gamma+\theta). \tag{19}$$

The completely inelastic collision at $-\gamma_{\max}$ that occurs when the moving ball passes from one line ball to the next defines the boundary conditions for the problem. We denote the velocity of the ball at $\gamma_{\max}$ by $v_t(\gamma_{\max})=v_i$. Since we assume rolling without slipping, on this ball on the line we have

$$v_i=\omega_i R, \tag{20}$$

with $\omega_i=\omega(\gamma_{\max})$. In the next instant, the moving ball hits the next ball on the line at $-\gamma_{\max}$, with the tangential velocity $v_t(-\gamma_{\max})$, which with respect to this ball is (due to the change in geometry)

$$v_t(-\gamma_{\max})=v_i\cos(2\gamma_{\max}). \tag{21}$$

In the collision that is now about to take place, the normal component

$$v_n(-\gamma_{\max})=v_i\sin(2\gamma_{\max}) \tag{22}$$

is reduced to zero, but this is not the whole effect of the collision. Since v_t dropped *before* the impact due to the change in geometry, but ω was left unaffected, at $-\gamma_{\max}$, there is excess rotational velocity and thus excess shear velocity v_s. If the frictional force is high enough (which we assume in this treatment), then the shear velocity at the point of contact should again be reduced to zero during the impact such that tangential and rotational velocities *after* the impact at $-\gamma_{\max}$, which we will denote by v_f and ω_f, respectively, fulfill the condition

$$v_f=\omega_f R. \tag{23}$$

During the impact at $-\gamma_{\max}$ the rotational and translational velocities thus adjust themselves, with only negligible energy loss (friction here mainly helps to distribute the excess rotational velocity to the translational degree of freedom, but, as the ball can rotate freely, dissipates only very little energy during the adjustment). Before the adjustment of rotational and translational velocities, the kinetic energy of the system was

$$E_{\rm kin}=\frac{1}{2}mv_i^2\cos^2(2\gamma_{\max})+\frac{1}{2}J\omega_i^2. \tag{24}$$

With Eqs. (16) and (23) we thus obtain from the energy balance the condition for v_f

$$\frac{1}{2}v_i^2\cos^2(2\gamma_{\max})+\frac{1}{2}J\omega_i^2=\frac{7}{10}mv_f^2. \tag{25}$$

Substituting ω_i according to Eq. (20), we get

$$v_f=v_i\sqrt{\frac{1}{7}[5\cos^2(2\gamma_{\max})+2]} \tag{26}$$

for the tangential velocity after the collision at $-\gamma_{\max}$. Since $v_t=(R+r)\dot{\gamma}$, this provides the boundary condition for Eq. (19).

We obtain $\overline{v}$ numerically by starting at $-\gamma_{\max}$ with an arbitrary and very high starting velocity $\dot{\gamma}_0$, letting the system evolve according to Eq. (19). Whenever $-\gamma_{\max}$ is reached, Eq. (26) is applied and we start again at $\gamma_{\max}$. We continue this process until either the ball rolls back (which we consider as trapping) or it reaches a steady state. The mean velocity in this steady state is plotted in Fig. 12, in comparison to simulation data for various coefficients of restitution. Clearly, the simulation for small e_n is closest to the theoretical curve (which assumes $e_n=0$), but also for higher e_n the approximation is still good.

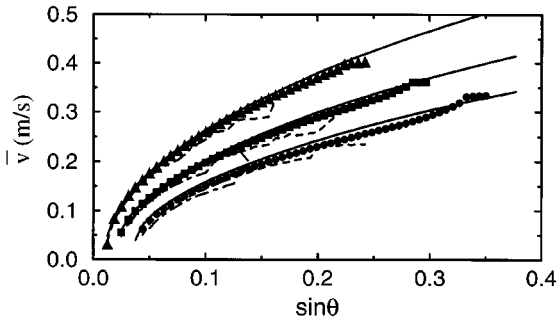

FIG. 12. Theoretical prediction of $\overline{v}$ (solid lines) for $\epsilon=0$ under the assumption $e_n=0$ and simulation data for $e_n=0.1$ and size ratios $\Phi=1.75$ (circles), 2.25 (squares), and 3.0 (triangles). The dashed and dot-dashed lines, respectively, also show the corresponding simulation data for $e_n=0.5$ and 0.7.

For the case $\epsilon>0$ Eqs. (19) and (26) yield equally good results as in the case $\epsilon=0$ presented in Fig. 12. In the case of a disordered line, an estimation of $\overline{v}$ with the value of $\gamma_{\max}$ chosen according to the mean value of ϵ fits the simulation results equally well.

Another result that can be obtained from this theoretical treatment is the phase boundary θ_{AB}. To this end, we make use of Eq. (18). By setting

$$E_{\rm kin}^0=\frac{7}{10}m(R+r)^2\dot{\gamma}^2(-\gamma_{\max}) \tag{27}$$

and

$$E_{\rm pot}^0=mg(R+r)\cos(\theta-\gamma_{\max}), \tag{28}$$

with the values at the beginning of the motion over one ball in the line and by using the fact that in the steady state

$$\dot{\gamma}(-\gamma_{\max})=e_t\dot{\gamma}(\gamma_{\max}), \tag{29}$$

with

$$e_t=\sqrt{\frac{1}{7}[5\cos^2(2\gamma_{\max})+2]}, \tag{30}$$

we obtain from Eq. (18) the starting velocity $\dot{\gamma}(-\gamma_{\max})$ in the steady state

$$\dot{\gamma}^2(-\gamma_{\max})=\frac{20}{7}\frac{g}{R+r}\frac{e_t^2}{1-e_t^2}\sin\gamma_{\max}\sin\theta. \tag{31}$$

We now assume that the phase boundary θ_{AB} is reached when the moving ball arrives at the angle $\gamma=-\theta$ with zero velocity, since from there it can roll down simply by the action of gravity, even zero starting velocity. For smaller

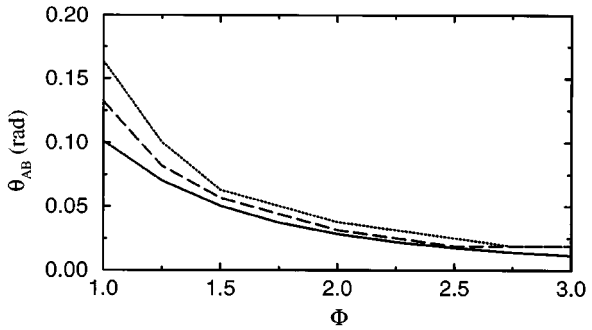

FIG. 13. Phase boundary θ_{AB} for $e_n=0.7$ (dotted line) and $e_n=0.1$ (dashed line) and the theoretical result from Eq. (34) for $e_n=0$.

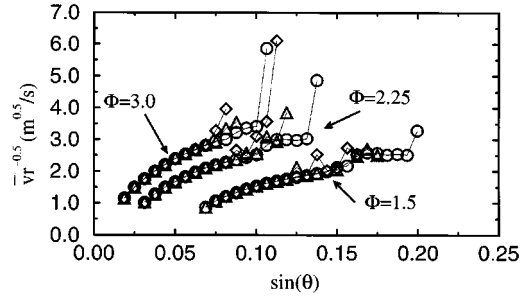

FIG. 14. Scaling of $\overline{v}$ with r keeping Φ constant. $r=0.5$ mm ($\diamond$), 1.25 mm ($\triangle$), and 5 mm ($\bigcirc$).

inclination angles, the ball would roll back before reaching this point and thus stop; for larger inclination angles it would pass this point with some velocity and move on. From Eq. (18) we obtain

$$\dot{\gamma}^2(-\gamma_{\max})=\frac{10}{7}\frac{g}{R+r}[1-\cos(\theta_{AB}-\gamma_{\max})] \qquad (32)$$

by setting $\gamma=-\theta_{AB}$ and $\dot{\gamma}(-\theta_{AB})=0$. If the ball is in region B, the steady-state condition (31) has to be fulfilled as well, so that from Eqs. (31) and (32) we get an equation for θ_{AB}

$$\frac{2e_t^2}{1-e_t^2}\sin\gamma_{\max}\sin\theta_{AB}=1-\cos(\theta_{AB}-\gamma_{\max}), \qquad (33)$$

which finally yields

$$\sin\theta_{AB}=\frac{\sin\gamma_{\max}}{\left(\frac{1+e_t^2}{1-e_t^2}\right)^2\sin^2\gamma_{\max}+\cos^2\gamma_{\max}} \times\left(\frac{1+e_t^2}{1-e_t^2}-\frac{2e_t}{1-e_t^2}\cos\gamma_{\max}\right). \qquad (34)$$

Figure 13 shows a comparison of this result to simulation data. Obviously, our theoretical result approximates the simulation results best for larger Φ. For Φ close to 1 the deviations get quite large, since here the assumption that the ball loses its normal velocity in a single impact is not fulfilled anymore as well as for larger Φ even for $e_n=0.1$. In any case, Eq. (34) provides a lower limit for the value of θ_{AB}.

After the completion of this work, we became aware of work by Ancey *et al.* [29] paralleling our theoretical treatment. They, however, neglect the effect of the rotational velocity in the impact at $-\gamma_{\max}$, though rotation is explicitly included in their equation of motion. They thus have to introduce a fitting parameter to match their curves to experimental data. This is not necessary if the influence of rotation is included in the boundary conditions of the problem, as we have shown. We emphasize that Eqs. (19) and (26) hold for the *instantaneous* velocity only in the case of vanishing normal restitution and perfectly rough surfaces, conditions that are not likely to be fulfilled by any commonly used material. However, as we have shown, the *mean* velocity of the ball is not influenced by the coefficients of restitution and friction and thus is correctly described.

One more result can be deduced directly from our theoretical treatment. Since $\dot{\gamma}\sim[r(\Phi+1)]^{-1/2}$ and $v_t=(\Phi+1)r\dot{\gamma}$, we expect $\overline{v}$ to scale with $\sqrt{r}$, i.e., to depend on the *absolute* size of the balls. Note that it does not, however, simply scale with $\sqrt{\Phi+1}$ as well, as Φ also enters the boundary conditions and thus changes $\dot{\gamma}$. But, keeping the geometry of the system (i.e., Φ and ϵ) constant, we expect a scaling of $\overline{v}$ with $\sqrt{r}$ in our simulations.

This scaling is observed in our simulations (see Fig. 14). In 2D experiments, it had been observed in an experimental setup restricted to $\Phi=1$ [15]; here we find it as well if we keep Φ fixed at an arbitrary value. This scaling seems to be quite universal since it was also found in 3D experiments [30] and in the 2D stochastic model [18].

V. SUMMARY AND DISCUSSION

We have discussed the mechanism stabilizing the motion of a ball on an inclined line consisting of equally sized balls. Two important results emerged from our simulations. First, we found that the motion of a ball in the steady state is very regular and consists of a series of small bounces on *each* ball on the line, contrary to what has been assumed so far [13,18]. In the course of these bounces the moving ball loses all relative normal velocity with respect to this ball. This dissipation mechanism holds both for lines with equally spaced balls and for lines with a random spacing of balls. Furthermore, the location of these bounces is the same on each ball, so that a random spacing of the balls on the line only smears out these locations a bit, but does not alter the motion significantly. Thus the velocity of the ball in the case of a random spacing of balls on the line can be approximated by the motion of the ball on an ordered line with appropriate spacing. The main reason for this regularity of the motion is that the moving ball has to climb over the top of every ball forming the line by a few bounces in the steady state. Since disorder only slightly changes the height to be climbed, it has only a small influence on the motion.

Clearly, this mechanism for keeping a constant velocity cannot hold in three dimenions, where there are a number of

ways for the ball to choose to go down the plane. The 3D case should be ruled by a competition between stability properties of the plane and the preferential direction given by the plane inclination and inertia of the moving ball. One might argue that introducing stronger disorder in the 2D case, for example, by using polydisperse balls on the line, would model a longitudinal section of the plane much closer. But this will not eliminate the strong dimensional difference between the 2D and 3D cases. In three dimenions, the moving ball, hitting a ball on the plane a little on the side (which would be one of the smaller balls in the 2D section), would be deflected towards the side, which in two dimensions is impossible. In the constant velocity regime in two dimensions on a line with size polydispersity, the moving ball will again lock into some kind of quasiperiodic behavior for the same reasons as explained above. The problem of having to overcome some maximum threshold (to get out of the deepest valley between two balls on the line) to keep moving is even stronger, contrary to the 3D case. There a ball, having suffered a large impact that greatly slows it down, might still find some way around the bump that slowed it and accelerate until the next impact via some statically unstable path. Thus the motion in three dimensions is expected to be far more irregular than can be modeled in two dimensions. Future simulations in three dimensions will have to show where these differences originate and what the stabilizing mechanism consists of in this case. A stochastic model for the 2D case [18,24] nevertheless showed a viscous friction force, i.e., a linear dependence of $\overline{v}$ on $\sin\theta$. This might be due to the fact that the randomness introduced there in the choice of the next impact captures the randomness of the ''real'' two-dimensional plane. However, this question can only be answered ultimately by 3D simulations.

The second important result is that material properties such as the normal coefficient of restitution e_n and the Coulomb friction coefficient μ hardly influence the mean velocity $\overline{v}$ in the steady state. From this result and the knowledge of the mechanism stabilizing the motion of the ball in two dimensions, we were able to predict $\overline{v}$ theoretically under the assumption of completely inelastic collisions. Only geometrical considerations sufficed for this treatment and gave a very good approximation to our simulation results. The results in this extreme case enabled us to derive a lower limit for the phase boundary θ_{AB}, which for large Φ gives a good approximation of θ_{AB} regardless of the value of the coefficient of restitution. This result should be relevant to the problem of segregation in the flow on inclined planes or in rotating drums.

Though we have made significant progress in understanding the stabilizing mechanism by which the ball keeps its constant velocity in two dimensions, a few open questions remain. Due to the strong nonlinearity of the problem (computation of successive impact angles, velocities, etc., from the equations of motion would require the solution of a fourth-order polynomial), a direct iteration of the equations of motions as for $e_n=0$ is very cumbersome, though in principle possible, in the case of nonvanishing e_n. Since the phase boundary θ_{BC}, which separates steady motion of the ball from the accelerating regime, depends on e_n, it cannot be derived directly from our theoretical treatment. The most obvious simplification one might introduce, namely, ignoring the structure of the plane in the computation of the next impact, is out of the question since we have found this structure to be essential for the stabilizing mechanism. The problem seems to be related to the classical problem of a ball bouncing on a vibrating plate [31], which lately has been discussed for the case of a partially inelastic ball [32]. In the case of finite restitution, it was found that neglecting the motion of the vibrating plate can lead to erroneous results, such as the observation of ''chaos'' in a region of phase space where a more exact treatment shows the existence of eventually periodic orbits. Unfortunately, even this simple one-dimensional problem can only be solved by approximations in the extreme cases $e_n \ll 1$ and $e_n \to 1$, so it is by no means obvious how to relate these results to our problem, since for these extreme cases, we already have solved the problem. (The case $e_n \to 1$ is trivial since there region B of the phase diagram vanishes.)

So for the 2D case, the remaining open questions are the following. So far, we do not understand well how the ball slows down to its stable velocity when it is launched on the plane with a much higher initial velocity or why it accelerates as soon as it bounces only approximately once per ball on the line. In addition, the questions of whether in the bouncing region a steady state is reached as well, as has been suggested before [13], and what the characteristics of this steady state are are of interest. Does the ball really move in a ''chaotic'' way in the bouncing regime, as is suspected [13], or might an eventually periodic motion exist as in the case of the ball on the vibrating plate, which due to the long transient so far could not be observed?

Although many of the interesting features of granular flow come about by the *collective* behavior and the interaction of many particles, we have shown that even the elementary processes involving only a single particle moving in a dissipative but fixed environment can offer insight and present new questions. One of these questions, which is also of relevance to granular flows in general, is that of dimensionality. It has always been implicitly assumed that two-dimensional model systems are an adequate tool to study granular flows in general, i.e., that the qualitative behavior will not be different in three dimensions. Our results show that even though this is probably true for behavior *in* the bulk, where grain motion is very confined, care has to be taken in relating the behavior on free surfaces in two dimensions to that in three dimensions.

ACKNOWLEDGMENTS

We wish to thank D. Bideau, I. Ippolito, L. Samson, and J. Schäfer for very valuable discussions. This work was supported in part by the Groupement de Recherche CNRS ''Physique des Milieux Hétérogènes Complexes'' and by the HCM European Network ''Cooperative Structures in Complex Media.''

[1] T. G. Drake, J. Geophys. Res. **95**, 8681 (1990).
[2] S. B. Savage and K. Hutter, J. Fluid Mech. **199**, 177 (1989).
[3] S. B. Savage, in *Disorder and Granular Media*, edited by D. Bideau and A. Hansen (Elsevier, Amsterdam, 1993).
[4] F. Cantelaube and D. Bideau, Europhys. Lett. **30**, 133 (1995).
[5] E. Clément, J. Rajchenbach, and J. Duran, Europhys. Lett. **30**, 7 (1995).
[6] O. Zik, D. Levine, S. G. Lipson, S. Strikman, and J. Stavans, Phys. Rev. Lett. **73**, 5 (1994).
[7] G. Baumann, I. M. Jánosi, and D. E. Wolf, Phys. Rev. E **51**, 1879 (1995).
[8] C. S. Campbell, Annu. Rev. Fluid Mech. **22**, 57 (1990).
[9] M. Caponeri, S. Douady, S. Fauve, and C. Laroche, in *Mobile Particulate Systems*, edited by E. Guazzelli and L. Oger (Kluwer, Dordrecht, 1995).
[10] O. Pouliquen and N. Renaut, J. Phys. (France) II **6**, 923 (1996).
[11] F.-X. Riguidel, R. Jullien, G. H. Ristow, A. Hansen, and D. Bideau, J. Phys. (France) I **4**, 261 (1994).
[12] F.-X. Riguidel, A. Hansen, and D. Bideau, Europhys. Lett. **28**, 13 (1994).
[13] G. H. Ristow, F.-X. Riguidel, and D. Bideau, J. Phys. (France) I **4**, 1161 (1994).
[14] A. Aguirre, I. Ippolito, A. Calvo, C. Henrique, and D. Bideau (unpublished).
[15] C. D. Jan, H. W. Shen, C. H. Ling, and C. I. Chen, in *Proceedings of the 9th Conference on Engineering Mechanics, College Station, Texas*, edited by L. D. Lutes and J. M. Niedzwecki (American Society of Civil Engineers, New York, 1992), p. 768.
[16] F.-X. Riguidel, Ph.D. thesis, Université de Rennes I, 1994 (unpublished).
[17] R. A. Bagnold, Proc. R. Soc. London Ser. A **225**, 49 (1954).
[18] G. G. Batrouni, S. Dippel, L. Samson, Phys. Rev. E **53**, 6496 (1996).
[19] M. P. Allen and D. J. Tildesley, *Computer Simulation of Liquids* (Clarendon, Oxford, 1987).
[20] P. A. Cundall and O. D. L. Strack, Géotechnique **29**, 47 (1979).
[21] J. Schäfer, S. Dippel, and D. E. Wolf, J. Phys. (France) I **6**, 5 (1996).
[22] S. F. Foerster, M. Y. Louge, H. Chang, and K. Allia, Phys. Fluids **6**, 1108 (1994).
[23] F. Radjai, J. Schäfer, S. Dippel, and D. E. Wolf, (unpublished).
[24] S. Dippel, L. Samson, and G. G. Batrouni, in *Proceedings of HLRZ Workshop on Traffic and Granular Flow*, edited by D. E. Wolf, M. Schreckenberg, and A. Bachem (World Scientific, Singapore, 1996).
[25] J. Schäfer and D. E. Wolf, Phys. Rev. E **51**, 6154 (1995).
[26] S. McNamara and W. R. Young, Phys. Fluids A **4**, 496 (1992).
[27] D. Bideau, I. Ippolito, L. Samson, G. G. Batrouni, S. Dippel, A. Aguirre, A. Calvo, and C. Henrique, in *Proceedings of HLRZ Workshop on Traffic and Granular Flow* (Ref. [24]).
[28] F. Radjai and S. Roux, Phys. Rev. E **51**, 6177 (1995).
[29] C. Ancey, P. Evesque, and P. Coussot, J. Phys. (France) I **6**, 725 (1996).
[30] L. Samson and I. Ippolito (private communication).
[31] M. A. Liebermann and A. J. Lichtenberg, Phys. Rev. A **5**, 1852 (1972).
[32] J. M. Luck and A. Mehta, Phys. Rev. E **48**, 3988 (1993).